ACS Medicinal Chemistry Letters

Letter

pubs.acs.org/acsmedchemlett

Discovery of a Potent, Selective, and Orally Available PI3Kδ Inhibitor for the Treatment of Inflammatory Diseases

Montse Erra,[*,†] Joan Taltavull,[†] Angelique Gréco,[†,⊥] Francisco Javier Bernal,[†] Juan Francisco Caturla,[†] Jordi Gràcia,[†] María Domínguez,[‡] Mar Sabaté,[‡] Stéphane Paris,[†] Salomé Soria,[†] Begoña Hernández,[†,▽] Clara Armengol,[§] Judit Cabedo,[∥] Mónica Bravo,[∥] Elena Calama,[∥] Montserrat Miralpeix,[∥] and Martin D. Lehner[∥,#]

[†]Medicinal Chemistry and Screening, [‡]Pharmacokinetics and Metabolism, [§]Systems Biology, and [∥]Respiratory Therapeutic Area, Almirall R&D, Barcelona 08980, Spain

Supporting Information

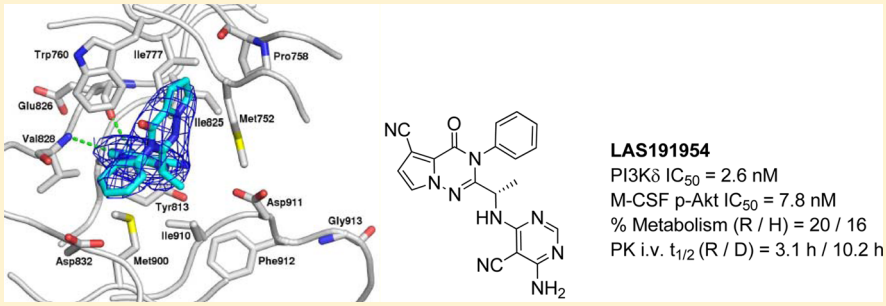

ABSTRACT: The delta isoform of the phosphatidylinositol 3-kinase (PI3Kδ) has been shown to have an essential role in specific immune cell functions and thus represents a potential therapeutic target for autoimmune and inflammatory diseases. Herein, the optimization of a series of pyrrolotriazinones as potent and selective PI3Kδ inhibitors is described. The main challenge of the optimization process was to identify an orally available compound with a good pharmacokinetic profile in preclinical species that predicted a suitable dosing regimen in humans. Structure−activity relationships and structure−property relationships are discussed. This medicinal chemistry exercise led to the identification of LAS191954 as a candidate for clinical development.

KEYWORDS: *Phosphoinositide-3-kinase delta inhibitor, PI3Kδ inhibitor, structure−activity relationship, autoimmune diseases, inflammatory diseases, lead optimization*

The phosphatidylinositol-3-kinase (PI3K) signal transduction pathway is central to a plethora of different cellular processes involving metabolism, proliferation, differentiation, or activation. Hence, manipulation of the PI3K pathway represents an interesting approach for treatment of a number of different pathological conditions such as cancer, where inhibitors of class IA PI3K with varying isoform selectivity profiles have already been established as treatment options for different indications.[1]

In the immune system, the PI3K delta isoform plays a central role in both innate and adaptive immune cell functions. Taking advantage of the strong dependency of B cells on functional PI3Kδ,[2] the oral PI3Kδ inhibitor Idelalisib has been successfully developed as a novel treatment for different types of B-cell malignancies.[3] In addition, the involvement of PI3Kδ in central immune functions suggests a therapeutic potential of PI3Kδ inhibitors as novel broad-acting anti-inflammatory agents for autoimmune diseases[4] and pathologies with an allergic or inflammatory component such as allergic rhinitis,[5] asthma,[6] or COPD.[7] Apart from inhibiting B cell activation, pharmacological inhibition of PI3K delta has been demonstrated to attenuate T cell receptor induced cytokine production,[8] to inhibit degranulation of basophils and mast cells,[5,9] and to suppress the oxidative burst response by neutrophils.[10] In addition, PI3Kδ seems to be involved in corticosteroid resistance induced by oxidative stress in macrophages,[11] thus indicating an activity profile complementary to other current treatments such as corticosteroids.

The discovery of the propeller-shaped inhibitor **1** (IC87114, ICOS) and the mechanisms by which δ isoform selectivity can be accomplished focused our attention.[12] Following this strategy, our efforts toward the identification of new PI3Kδ inhibitors were based on a pyrrolotriazinone scaffold as shown in Scheme 1. Our initial lead **2** showed similar PI3Kδ inhibitor potency to IC87114 (110 nM versus 130 nM) and also high selectivity against the other class I PI3K isoforms. Moving the methyl group from the phenyl ring in compound **2** to the linker (compound **3**), slightly improved the PI3Kδ inhibitor potency to 75 nM and

Received: November 3, 2016
Accepted: November 30, 2016
Published: November 30, 2016

DOI: 10.1021/acsmedchemlett.6b00438
ACS Med. Chem. Lett. 2017, 8, 118−123

Scheme 1. Pyrrolotriazinone Scaffold

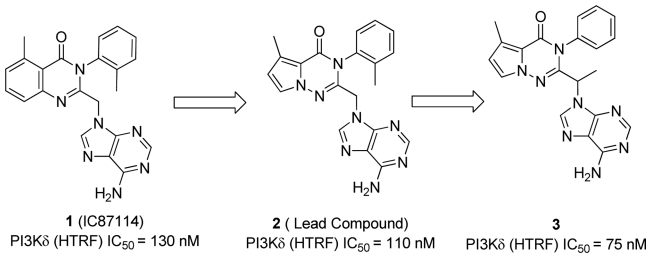

removed the potential for atropisomerism[13] present in ortho-substituted compounds **1** and **2**. Taking into account the stereochemistry of known PI3Kδ selective inhibitors in the clinic such as Idelalisib[14] and Duvelisib,[15] the *S*-enantiomers were initially targeted.

Thus, an extensive structure−activity relationship (SAR) study was then performed around compound **3** to improve the potency and modulate ADME properties.

Most kinase inhibitors are known to bind to a region in the kinase termed the hinge binder region, usually with an H-bond acceptor−donor pair. Initially, an exploration of this region was undertaken, and PI3Kδ inhibitory potency in both enzymatic and cellular assays was assessed together with *in vitro* metabolism[16] for each compound (Table 1). Introduction of other purine-like hinge binders (**4**, **5**) increased the *in vitro* potency for PI3Kδ considerably, and the compounds showed low *in vitro* metabolism. Other bicyclic rings (**6**−**8**) demonstrated lower potency and decreased metabolic stability when compared to compounds **4** and **5**. Monocyclic rings such as those in compounds **9**−**13** (Table 1) were then studied and cyanopyrimidine **11** showed the best overall balance between potency and *in vitro* metabolism. A clear correlation between metabolism rate and lipophilicity could not be established; however, a tendency was observed for those compounds with a $cLogD_{7.4}$ around 2.0 or above all showing low metabolic stability.

Optimization of the linker was then explored as shown in Table 2. An ethyl group was well tolerated giving a compound (**14**) of similar potency to the methyl derivative **4** but poorer microsomal stability. The corresponding (*R*)-enantiomer of **14** was synthesized (compound **15**) and the resultant drop off in potency confirmed the preference of PI3Kδ for the (*S*)-enantiomer. Replacing the hinge binder of compound **14** for the cyanopyrimide (**16**) slightly improved potency and *in vitro* metabolism. Appending a hydroxyl group onto compounds **11** and **16** resulted in derivative **18** and **17**, respectively, but only compound **17** showed an improved microsomal stability while maintaining good PI3Kδ potency. In contrast, introduction of a trifluoroethyl group (compound **19**) was less well tolerated. Cyclic analogue **20** kept *in vitro* potency but was metabolically less stable. Introduction of fluorine atoms in the cyclopentyl ring of **20** with the aim of increasing metabolic stability led to a less potent compound **21**. Spirocyclic ring variation (compound **22**) resulted in a large drop off in potency.

Compounds **11** and **17** were then profiled in a rat *in vivo* pharmacokinetic (PK) experiment. However, for both compounds, *in vivo* clearance in rat was higher than expected from the microsomal stability data, resulting in moderate systemic exposure and short half-lives (Table 3).

To better understand the binding mode of the ligands an X-ray cocrystal of human PI3Kδ in complex with compound **11** was performed. The structure was solved at a resolution of 2.85 Å,

Table 1. SAR Exploration of the Hinge Binder[a]

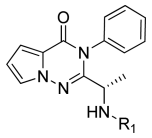

Compd	R_1	PI3Kδ (HTRF)[b] IC_{50} (nM)	M-CSF p-Akt[c] IC_{50} (nM)	% Metabolism (rat/human)[d]	$cLogD_{7.4}$[e]
4		10	7	18 / 30	1.5
5	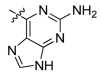	3.1	6.5	30 / 26	1.3
6		60	-	100 / 86	2.0
7		52	150	44 / 49	2.3
8		9	47	48 / 58	2.5
9		73	210	-	1.8
10		12	-	51 / 43	2.5
11		4.3	4.7	15 / 24	1.5
12	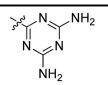	91	76	25/ 33	0.8
13		1200	-	-	1.5

[a]All assay results are reported as the geometric mean of at least two separate runs. [b]PI3Kδ activities were measured with an ATP concentration fixed at the K_m of PI3Kδ by HTRF, where the PIP3 product is detected by displacement of biotin-PIP3 from an energy transfer complex. [c]THP-1 cells were treated with compounds for 30 min, stimulated with M-CSF at EC_{80} for 3 min, and then lysed to measure (by ELISA) pAkt (Thr308) produced through PI3Kδ. [d]Percent metabolism expressed as disappearance of parent compound after microsomal incubation for 30 min (1 mg/mL protein and 5 μM compound at 37 °C). [e]Calculated LogD value at pH = 7.4.

revealing the detailed binding mode of the ligand. Like IC87114, compound **11** adopted a propeller-shaped conformation where the pyrrolotriazinone moiety was sandwiched into the induced hydrophobic specificity pocket between Trp760 and Met752. The cyanopyrimidine ring of **11** served as the hinge binder and formed two specific hydrogen bonds to the main chain atoms of Val828 and Glu826. The following residues were found in the vicinity of the ligand with a maximum distance of 3.9 Å: Met752, Pro758, Trp 760, Ile777, Tyr813, Ile825, Glu826, Val827, Val828, Ser831, Asp832, Met900, Ile910, and Asp911. A closer look at the binding pocket surface (Figure 1) suggested that the pyrrolotriazinone core ring could be substituted at the 5-, 6- or 7-position to further modulate potency.

DOI: 10.1021/acsmedchemlett.6b00438
ACS Med. Chem. Lett. 2017, 8, 118−123

Table 2. Linker SAR Exploration[a]

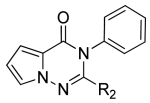

Compd	R_2	PI3Kδ (HTRF)[b] IC_{50} (nM)	M-CSF p-Akt[c] IC_{50} (nM)	% Metabolism (rat/human)[d]
14	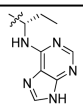	25	-	38 / 49
15	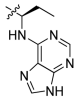	1800	-	32 / 30
16	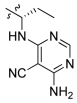	11	18	32 / 32
17	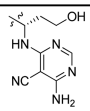	4.8	16	ND / 7
18	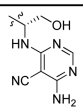	13	51	24 / 31
19	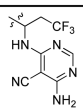	610	1600	-
20	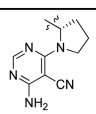	4.6	6.6	46 / 48
21	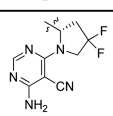	31	370	30 / 35
22	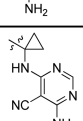	3400	-	-

[a]All assay results are reported as the geometric mean of at least two separate runs. [b]PI3Kδ activities were measured with an ATP concentration fixed at the K_m of PI3Kδ by HTRF, where the PIP3 product is detected by displacement of biotin-PIP3 from an energy transfer complex. [c]THP-1 cells were treated with compounds for 30 min, stimulated with M-CSF at EC_{80} for 3 min, and then lysed to measure (by ELISA) pAkt (Thr308) produced through PI3Kδ. [d]Percent metabolism expressed as disappearance of parent compound after microsomal incubation for 30 min (1 mg/mL protein and 5 μM compound at 37 °C).

Table 3. Rat PK Profiles of Compounds 11 and 17

compd	$t_{1/2}$ (h)[a]	AUC (ng·h/mL)[a]	Cl (mL/min/kg)[a]	Vss (L/kg)[a]
11	0.9	386	43.5	1.9
17	1.1	450	36.8	1.6

[a]Mean values (n = 2) in Wistar rat after an administration of 1 mg/kg i.v. Parameters calculated from plasma samples: $t_{1/2}$ = half-life, Cl = clearance, AUC = area under the curve, Vss = volume of distribution at steady state.

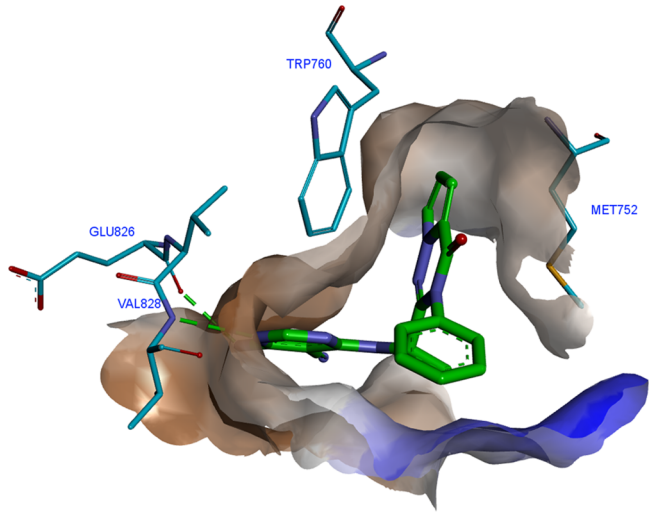

Figure 1. X-ray cocrystal structure of the binding pocket surface of human PI3Kδ containing compound **11**.

Thus, several analogues with different substitutions on the pyrrolo ring were synthesized and tested. A methyl group was well tolerated in different positions (compounds **23** and **29**), but the resultant derivatives were metabolically unstable (Table 4). Appending a hydroxyl group onto the methyl group of **23** resulted in a compound **24** with reasonable PI3Kδ inhibitor potency and improved metabolic stability. After further study it was found that placement of other substituents at position 5 (**25**, **26**, and **27**) gave rise to compounds with excellent potencies and good metabolic stability. Further characterization of compound **25** showed the formation of GSH adducts following incubation of **25** with microsomes in the presence of glutathione (GSH). As the formation of reactive metabolites is potentially involved in severe adverse drug reactions, this compound was not further profiled. Moving this fluorine atom to position 6 (compound **28**) slightly diminished potency. At position 7, compounds bearing small groups such as methyl (**29**) or cyano (**30**) were better tolerated than a bulkier trifluoromethyl group (**31**). Finally, the imidazotriazinone **32** showed a substantially diminished PI3Kδ inhibitor potency in comparison to the corresponding pyrrolotriazinone **11**.

From this set of compounds, **26** and **27** were further profiled in a rat *in vivo* PK experiment (Table 5) to determine if the *in vitro* metabolism results were, in these cases, predictive of the *in vivo* clearance values. These results were compared with Idelalisib, the most advanced compound in clinical development at that moment.

As seen in Table 5, compounds **26** and **27**, with substituents at position 5 of the pyrrolo ring, showed increased plasma exposure compared to unsubstituted compounds **11** and **17**, excellent oral bioavailability and reduced clearance in rat, which was more consistent with the observed microsomal stability values. One plausible hypothesis could be that, although moderate metabolism was observed for unsubstituted pyrrolo derivatives such as **11** and **17**, many metabolites (>5) were identified after microsomal incubation for both compounds and those metabolites might be magnified *in vivo*. The same behavior was observed for Idelalisib, a compound also showing moderate *in vitro* metabolism (20% and 21% in rat and human liver microsomes, respectively) with seven metabolites identified. In contrast, compounds with substitution on the pyrrolo ring formed fewer metabolites in microsomes (except for compounds

DOI: 10.1021/acsmedchemlett.6b00438
ACS Med. Chem. Lett. 2017, 8, 118−123

Table 4. Distal Core SAR Exploration[a]

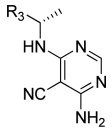

Compd	R_3	PI3Kδ (HTRF)[b] IC_{50} (nM)	M-CSF p-Akt[c] IC_{50} (nM)	% Metabolism (rat/human)[d]
23	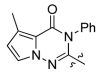	1.1	1.6	44 / 80
24	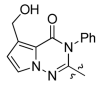	4.3	35	7 / 23
25	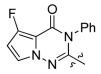	1.1	3.8	9 / 13
26 LAS191954	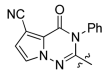	2.6	7.8	20 / 16
27	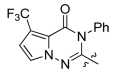	3.0	3.0	16 / 37
28	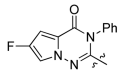	17	51	23 / 34
29	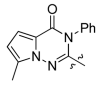	8.8	11	54 / 82
30	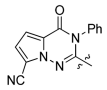	4.0	11	24 / 22
31	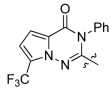	71	380	-
32	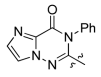	57	210	14 / 23

[a]All assay results are reported as the geometric mean of at least two separate runs. [b]PI3Kδ activities were measured with an ATP concentration fixed at the K_m of PI3Kδ by HTRF, where the PIP3 product is detected by displacement of biotin-PIP3 from an energy transfer complex. [c]THP-1 cells were treated with compounds for 30 min, stimulated with M-CSF at EC_{80} for 3 min and then lysed to measure (by ELISA) pAkt (Thr308) produced through PI3Kδ. [d]Percent metabolism expressed as disappearance of parent compound after microsomal incubation for 30 min (1 mg/mL protein and 5 μM compound at 37 °C).

Table 5. Rat PK Profiles of Compounds 26 and 27 in Comparison with Idelalisib

compd	$t_{1/2}$ (h)[a]	AUC (ng·h/mL)[a]	Cl (mL/min/kg)[a]	Vz (L/kg)[a]	F (%)[b]
Idelalisib	0.8	512	32.8	2.2	68
26	3.1	1729	9.6	2.6	101
27	3.3	2040	8.6	2.4	113

[a]Mean values (n = 2) in Wistar rat after an administration of 1 mg/kg i.v. [b]Mean values (n = 2) in Wistar rat after an administration of 1 mg/kg p.o.

bearing a methyl group), and this could explain the lower clearance observed *in vivo*.

Additionally, the PK properties of both compounds **26** and **27** were studied in dog as a second preclinical species to allow for estimation of the human half-life based on allometric scaling. The dog *in vivo* PK data are shown in Table 6. Both compounds **26** and **27** displayed a superior PK profile to Idelalisib in the two preclinical species. Compound **26** (LAS191954), with excellent oral bioavailability and low clearance in the two species, gave a superior predicted half-life in humans and was further profiled.

For the assessment of selectivity, the enzymatic potency of LAS191954 on the four class I PI3K recombinant human isoforms was determined by HTRF with a compound preincubation time of 30 min. Assays were run at ATP concentration equal to the respective K_m and using a subnanomolar concentration of the enzyme. In these conditions, LAS191954 showed a potency on the target of 2.6 nM, with the highest selectivity versus PI3Kα (8.2 μM) and the lowest versus PI3Kγ and PI3Kβ (72 and 94 nM, respectively). The compound was then tested in a primary PI3Kδ-dependent cellular assay based on M-CSF-induced AKT phosphorylation, a downstream effector of PI3Kδ, in the human monocytic cell line THP-1. An IC_{50} of 7.8 nM was obtained indicating that the compound had excellent permeability and cellular activity. To evaluate the cellular inhibition of PI3Kβ, an assay based on stimulation of HUVEC cells with sphingosine-1-P was employed.[17] The results (IC_{50} = 295 nM) indicated that the enzymatic selectivity between δ and β isoforms (36-fold) was maintained at the cell-based level (38-fold). The compound was also selective against an extensive panel of protein and lipid kinases and GPCRs.

PI3Kδ kinase is involved in the activation of B cells upon antigen binding to the B cell receptor (BCR),[18] and thus, inhibitors of PI3Kδ are expected to inhibit BCR activation. The effect of LAS191954 on the function of human B cells was assessed *in vitro* by cross-linking the B-cell receptor with anti-IgD antibodies and assessing the early activation marker CD69 in the CD19+ B cell subset by flow cytometry. On isolated PBMC, LAS191954 showed an IC_{50} of 4.6 nM. Similar assay performed in human whole blood yielded an IC_{50} of 47 nM.

From an ADME perspective, further *in vitro* characterization of LAS191954 was performed as summarized in Table 7. Plasma protein binding[19] was low in preclinical species (60−65% in mouse/rat/dog) in contrast to human (95%), which might be the major factor accounting for the difference in potency between the isolated human PBMC and whole blood assays previously described. The compound showed a good permeability[20] and did not show any signs of plasma instability. Drug−drug interactions are not expected in a clinical setting since neither inhibition nor induction of the major CYP450 isoforms was observed in vitro in humans. Opposite to compound **25**, no formation of GSH-adducts was observed following incubation of LAS191954 with rat and human liver microsomes in the presence of glutathione (GSH).

In terms of cardiac safety, LAS191954 did not show any activity on the hERG channel up to 10 μM.

As a consequence of these encouraging results, the compound was further characterized in different *in vivo* models.

PI3Kδ has been implicated in T-cell proliferation *in vitro* and *in vivo*. Cytokine production induced by concanavalin A (ConA) or anti-CD3 antibody activation of naïve CD4+ T cells in mice is blocked by PI3Kδ inhibition.[21] To assess the effect of LAS191954 on T cell cytokine production *in vivo*, a rat model of ConA induced IL2 production was employed in which the compound was administered orally 1 h prior to an intravenous ConA challenge (10 mg/kg) and IL2 levels were measured 90

DOI: 10.1021/acsmedchemlett.6b00438
ACS Med. Chem. Lett. 2017, 8, 118−123

Table 6. Dog PK Profiles of Compounds 26 and 27 in Comparison with Idelalisib

compd	$t_{1/2}$ (h)[a]	AUC (ng·h/mL)[a]	Cl (mL/min/kg)[a]	Vz (L/kg)[a]	F (%)[b]
Idelalisib	1.6	924	21.5	2.5	
26	10.2	9441	1.4	1.2	98
27	4.2	3937	4.2	1.5	

[a]Mean values (n = 2) in Beagle dog after an administration of 1 mg/kg i.v. [b]Mean values (n = 3) in Beagle dog after an administration of 1 mg/kg p.o.

Table 7. *In Vitro* ADME Profile of LAS191954

human PPB (% bound)[a]	PAMPA P_{app} ($\times 10^{-6}$ cm/s)[b]	plasma stability (24 h)[c]	CYP450 inhibition[d]	CYP450 induction[e]
95.4	2.8	100%	>25 μM	No issues

[a]Mean PPB values determined by equilibrium dialysis at a plasma concentration of 1 μM at 37 °C. [b]Permeability values at RT in PBS (containing 2% DMSO),; compound concentration in donor compartment: 20 μM. [c]LAS191954 stability at 37 °C at 2 μg/mL in plasma (anticoagulant: sodium heparin). [d]CYP450 in HLM with and without preincubation for CYP1A2, 3A4, 2D6, 2C9, and 2C19 isoforms. [e]Induction of CYP1A and 3A4 isoforms was assessed in cultured human cryopreserved hepatocytes at concentrations up to 50 μM.

min later. LAS191954 inhibited IL2 production with an ID_{50} of 0.13 mg/kg as compared to an ID_{50} of 1.6 mg/kg of Idelalisib as shown in Figure 2.

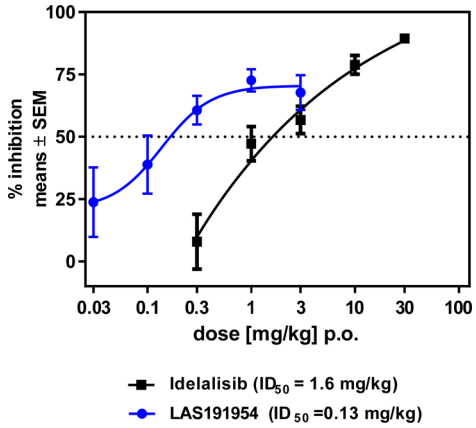

Figure 2. Inhibition of ConA induced increase in IL-2 levels in rat plasma of LAS191954 vs reference compound Idelalisib.

PI3Kδ participates in the proliferation, differentiation, migration, and cytokine production of T lymphocytes, in the migration and release of ROS and proteases by neutrophils, and in the migration, alternative M2 activation, and loss of steroid sensitivity of macrophages. PI3Kδ additionally regulates Fcε mediated mast cell and basophil degranulation. Thus, the anti-inflammatory efficacy of LAS191954 was assessed in an airway allergic inflammation model characterized by infiltration of eosinophils to the alveolar compartment in response to ovalbumin challenge in previously sensitized Brown Norway rats.

A twice daily administration of LAS191954 1 h prior to and 6 h post-ovalbumin (OVA) challenge dose-dependently reduced the number of eosinophils in the bronchoalveolar lavage (BAL) at 24 h in rat with an ID_{50} of 0.16 mg/kg. The reference compound Idelalisib, administered also twice daily, displayed a considerably lower potency with an ID_{50} of 15 mg/kg (Figure 3).

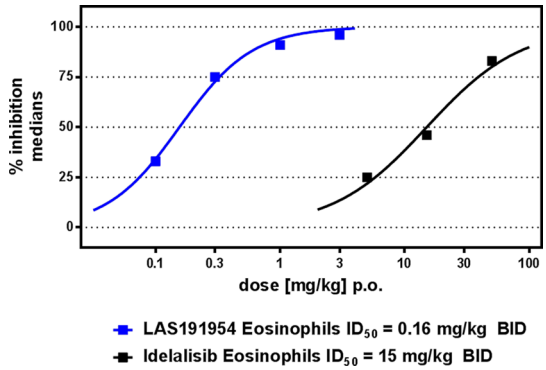

Figure 3. Inhibition of OVA BAL cell accumulation in BN rats at 24 h by twice daily doses of LAS191954 and Idelalisib.

In both in vivo models LAS191954 showed efficacy at significantly lower doses than Idelalisib. These results could not be explained by differences in *in vitro* potency as Idelalisib exhibited a similar cellular PI3Kδ inhibitor potency with an IC_{50} of 7.6 nM, but they are in accordance with a superior PK profile (higher systemic exposure and longer half-life) of LAS191954 in rat.

In summary, a new series of potent and selective PI3Kδ inhibitors has been identified. The SAR exercise focused on optimizing both the *in vitro* potency and the ADME profile of the compounds in order to find a potentially once-a-day drug. The pyrrolotriazinone scaffold enabled us to build in better pharmacokinetic properties in preclinical species, which may ultimately translate in a compound with reduced dosing in humans, and culminated in the identification of LAS191954 as a candidate for clinical development.

■ ASSOCIATED CONTENT

Supporting Information

The Supporting Information is available free of charge on the ACS Publications website at DOI: 10.1021/acsmedchemlett.6b00438.

Characterization of all compounds. Experimental procedures for the sequence leading to key compound **26**. Description of all biological assays and in vivo studies. Crystallographic data collection and refinement statistics for crystal structure of compound **11** (PDF)

Accession Codes

PDB code for X-ray crystal structure described in this study has been deposited in the Protein Data Bank under the following accession codes: 5M6U (compound **11** in complex with PI3Kδ).

■ AUTHOR INFORMATION

Corresponding Author

*Phone: + 34 93 312 87 14. E-mail: montse.erra@almirall.com.

DOI: 10.1021/acsmedchemlett.6b00438
ACS Med. Chem. Lett. 2017, 8, 118−123

Present Addresses

[⊥]Pharmaxis Ltd., 20 Rodborough Road, Frenchs Forest, NSW 2086, Australia.

[#]Bionorica SE, Kerschensteinerstraße 11−15, 92318 Neumarkt, Germany.

[▽]Fundació ACE, Marqués de Sentmenat, 57, 08029 Barcelona, Spain.

Author Contributions

The manuscript was written through contributions of all authors. All authors have given approval to the final version of the manuscript.

Notes

The authors declare no competing financial interest.

■ ACKNOWLEDGMENTS

The authors wish to thank Proteros Biostructures GmbH for X-ray structure determination of human PI3Kδ in complex with compound **11** (PDB code: 5M6U). We also acknowledge the significant technical support provided by Jordi Sanahuja, Gaspar Casals, and Antonia Molina. We thank Sonia Espinosa and Josep M. Huerta for their support on physicochemical properties analysis and structural characterization of compounds.

■ REFERENCES

(1) Stark, A.; Sriskantharajah, S.; Hessel, E. M.; Okkenhaug, K. PI3K inhibitors in inflammation, autoimmunity and cancer. *Curr. Opin. Pharmacol.* **2015**, *23*, 82−91.

(2) Puri, K. D.; Gold, M. R. Selective inhibitors of phosphoinositide 3-kinase delta: modulators of B-cell function with potential for treating autoimmune inflammatory diseases and B-cell malignancies. *Front. Immunol.* **2012**, *3*, 256.

(3) Cheah, C. Y.; Fowler, N. H. Idelalisib in the management of lymphoma. *Blood* **2016**, *128* (3), 331−6.

(4) Durand, C. A.; Richer, M. J.; Brenker, K.; Graves, M.; Shanina, I.; Choi, K.; Horwitz, M. S.; Puri, K. D.; Gold, M. R. Selective Pharmacological Inhibition of Phosphoinositide 3-Kinase p110delta Opposes the Progression of Autoimmune Diabetes in Non-Obese Diabetic (NOD) Mice. *Autoimmunity* **2013**, *46* (1), 62−73.

(5) Horak, F.; Puri, K. D.; Steiner, B. H.; Holes, L.; Xing, G.; Zieglmayer, P.; Zieglmayer, R.; Lemell, P.; Yu, A. Randomized Phase 1 study of the phosphatidylinositol 3-kinase δ inhibitor Idelalisib in patients with allergic rhinitis. *J. Allergy Clin. Immunol.* **2016**, *137* (6), 1733−41.

(6) Rowan, W. C.; Smith, J. L.; Affleck, K.; Amour, A. Targeting phosphoinositide 3-kinase δ for allergic asthma. *Biochem. Soc. Trans.* **2012**, *40* (1), 240−5.

(7) Sriskantharajah, S.; Hamblin, N.; Worsley, S.; Calver, A. R.; Hessel, E. M.; Amour, A. Targeting phosphoinositide 3-kinase δ for the treatment of respiratory diseases. *Ann. N. Y. Acad. Sci.* **2013**, *1280*, 35−9.

(8) Soond, D. R.; Bjørgo, E.; Moltu, K.; Dale, V. Q.; Patton, D. T.; Torgersen, K. M.; Galleway, F.; Twomey, B.; Clark, J.; Gaston, J. S.; Taskén, K.; Bunyard, P.; Okkenhaug, K. PI3K p110delta regulates T-cell cytokine production during primary and secondary immune responses in mice and humans. *Blood* **2010**, *115* (11), 2203−2213.

(9) Ali, K.; Camps, M.; Pearce, W. P.; Ji, H.; Rückle, T.; Kuehn, N.; Pasquali, C.; Chabert, C.; Rommel, C.; Vanhaesebroeck, B. Isoform-Specific Functions of Phosphoinositide 3-Kinases: p110δ Not p110γ Promotes Optimal Allergic Responses In Vivo. *J. Immunol.* **2008**, *180* (4), 2538−2544.

(10) Fung-Leung, W. P. Phosphoinositide 3-kinase delta (PI3Kδ) in leukocyte signaling and function. *Cell. Signalling* **2011**, *23* (4), 603−8.

(11) Marwick, J. A.; Caramori, G.; Casolari, P.; Mazzoni, F.; Kirkham, P. A.; Adcock, I. M.; Chung, K. F.; Papi, A. A role for phosphoinositol-3-kinase delta in the impairment of glucocorticoid responsiveness in patients with chronic obstructive pulmonary disease. *J. Allergy Clin. Immunol.* **2010**, *125* (5), 1146−53.

(12) Berndt, A.; Miller, S.; Williams, O.; Le, D. D.; Houseman, B. T.; Pacold, J. I.; Gorrec, F.; Hon, W.-C.; Liu, Y.; Rommel, C.; Gaillard, P.; Ruckle, T.; Schwarz, M. K.; Shokat, K. M.; Shaw, J. P.; Williams, R. L. The p110δ structure: mechanisms for selectivity and potency of new PI(3)k inhibitors. *Nat. Chem. Biol.* **2010**, *6* (2), 117−124.

(13) Evarts, J. B.; Ulrich, R. G. Atropisomers of PI3K-inhibiting compounds. WO2012/040634.

(14) Somoza, J. R.; Koditek, D.; Villaseñor, A. G.; Novikov, N.; Wong, M. H.; Liclican, A.; Xing, W.; Lagpacan, L.; Wang, R.; Shultz, B. E.; Papalia, G. A.; Samuel, D.; Lad, L.; McGrath, M. E. Structural, Biochemical, and Biophysical Characterization of Idelalisib Binding to Phosphoinositide 3-Kinase δ. *J. Biol. Chem.* **2015**, *290* (13), 8439−8446.

(15) Winkler, D. G.; Faia, K. L.; DiNitto, J. P.; Ali, J. A.; White, K. F.; Brophy, E. E.; Pink, M. M.; Proctor, J. L.; Lussier, J.; Martin, C. M.; Hoyt, J. G.; Tillotson, B.; Murphy, E. L.; Lim, A. R.; Thomas, B. D.; Macdougall, J. R.; Ren, P.; Liu, Y.; Li, L.; Jessen, K. A.; Fritz, C. C.; Dunbar, J. L.; Poter, J. R.; Rommel, C.; Palombella, V. J.; Changelian, P. S.; Kutok, J. L. PI3K-δ and PI3K-γ inhibiton by IPI-145 abrogates immune responses and suppresses activity in autoimmune and inflammatory disease models. *Chem. Biol.* **2013**, *20* (11), 1364−74.

(16) McGinnity, D. F.; Soars, M. G.; Ubanowicz, R. A.; Riley, R. J. Evaluation of fresh and cryopreserved hepatocytes as in vitro drug metabolism tools for the prediction of metabolic clearance. *Drug Metab. Dispos.* **2004**, *32*, 1247−1253.

(17) Heller, R.; Chang, Q.; Ehrlich, G.; Hsieh, S. N.; Schoenwaelder, S. M.; Kuhlencordt, P. J.; Preissner, K. T.; Hirsch, E.; Wetzker, R. Overlapping and distinct roles for PI3Kβ and γ isoforms in S1P-induced migration of human and mouse endothelial cells. *Cardiovasc. Res.* **2008**, *80*, 96−105.

(18) Dal Porto, J. M.; Gauld, S. B.; Merrel, K. T.; Mills, D.; Pugh-Bernard, A. E.; Cambier, J. B cell antigen receptor signaling 101. *Mol. Immunol.* **2004**, *41* (6−7), 599−613.

(19) Banker, M. J.; Clark, T. H.; Williams, J. A. Development and validation of 96Well Equilibrium dialysis apparatus for measuring plasma protein binding. *J. Pharm. Sci.* **2003**, *92* (5), 967−974.

(20) Wohnsland, F.; Faller, B. High-throughput permeability pH profile and high-throughput alkane/water log P with artificial membranes. *J. Med. Chem.* **2001**, *44* (6), 923−30.

(21) Soond, D. R.; Slack, E. C. M.; Garden, O. A.; Patton, D. T.; Okkenhaug, K. Does the PI3K pathway promote or antagonize regulatory T cell development and function? *Front. Immunol.* **2012**, *3*, 244.

DOI: 10.1021/acsmedchemlett.6b00438
ACS Med. Chem. Lett. 2017, 8, 118−123